ELSEVIER

J. Non-Newtonian Fluid Mech. 111 (2003) 199–209

Journal of Non-Newtonian Fluid Mechanics

www.elsevier.com/locate/jnnfm

The flow of non-Newtonian fluids around bubbles and its connection to the jump discontinuity

J.R. Herrera-Velarde[a], R. Zenit[b,*], D. Chehata[b], B. Mena[b]

[a] *Instituto Tecnológico de Zacatepec, Av. Instituto Tecnológico No. 27, Zacatepec Morelos 67980, México*

[b] *Instituto de Investigaciones en Materiales, Universidad Nacional Autónoma de México, Apdo. Postal 70-360, Cd. Universitaria, Coyoacán, México DF 04510, México*

Received 6 June 2002; received in revised form 27 December 2002; accepted 18 February 2003

Abstract

The flow field around air bubbles rising in aqueous polyacrylamide (PAAm) solutions was studied using a particle image velocimetry (PIV) system. This flow was analyzed in the vicinity of the critical bubble volume where the discontinuity of the terminal bubble velocity occurs. It was found that the flow configuration changes drastically below and above the critical bubble volume. The flow just below the critical bubble volume shows an upward flow at the front and back of the bubble with a symmetrical vortex around the bubble. The flow field obtained for a volume just above the critical one shows the appearance of the so-called negative wake behind the bubble. Additionally, it was found that the container walls affect significantly the magnitude of the terminal velocity as well as the velocity jump. However, the critical volume at which the velocity jump appears does not change for different container sizes.

Keywords: Bubble velocity; Jump discontinuity; Viscoelastic liquid; Shear-thinning fluid; Particle image velocimetry

1. Introduction

Flows of non-Newtonian liquids show several interesting phenomena. Rod-climbing, die extrudate and tubeless siphon are just few typical examples of such peculiar phenomena. A list and explanations of some of these phenomena in non-Newtonian flows can be found in [1]. There are a number of interesting effects for the case of the motion of gas bubbles in non-Newtonian liquids. It must be noted that an understanding of many of these peculiar behaviors is rather limited [2,3]. For example, the Uebler effect [4] shows that a bubble may come to a sudden stop in contraction flows of viscoelastic fluids. As opposed to what is observed in Newtonian flows, bubbles in non-Newtonian

* Corresponding author. Tel.: +52-55-5622-4593; fax: +52-55-5616-1201.
E-mail address: zenit@servidor.unam.mx (R. Zenit).

0377-0257/03/$ – see front matter
doi:10.1016/S0377-0257(03)00055-7

liquids adopt teardrop shapes [5]. Hassager [6] found that the liquid velocity behind bubbles rising in a non-Newtonian liquid forms a *negative wake*. Astarita and Apuzzo [7] reported that as the bubble size increases, a sudden jump of the bubble terminal velocity is observed. They attributed this discontinuity to the elasticity of the fluid. Rodrigue et al. [8,9] experimentally demonstrated that surface tension as well as elastic forces must be simultaneously present, in order to generate a sudden jump in the velocities. All the studies reported to date, have only shown the flow field around bubbles rising in non-Newtonian fluids for bubbles with volumes above the critical volume discontinuity [3,6,10,11]. The flow around spheres moving in elastic and viscoelastic fluids has also been studied recently using particle image velocimetry (PIV) [12,13]. The appearance of the so-called negative wake is also observed for the flow around solid spheres for a wide range of Deborah numbers.

In the present study, we found that the velocity field around the bubble changes significantly for bubble volumes just below and above the critical volume where the velocity discontinuity occurs. Measurements of the mean bubble velocity were obtained using a high-speed camera. The velocity field around the bubbles was obtained using a PIV system. Additionally, we found that the magnitude of the jump discontinuity is greatly affected by the size of the container in which the experiments are carried out.

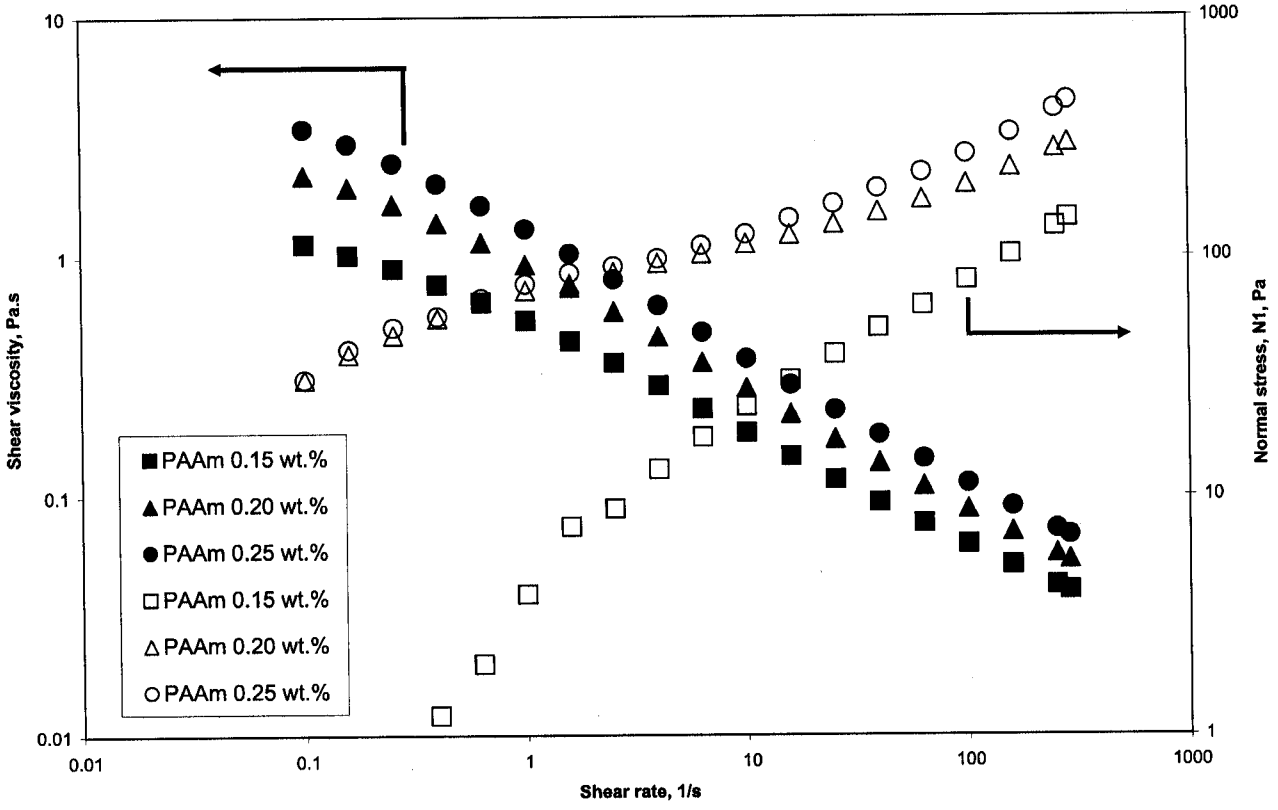

Fig. 1. Variation of the viscosity and first normal stress difference N1 of PAAm solutions vs. shear rate.

2. Experimental

A preliminary set of experiments was performed to measure the rise bubble velocity and to determine the critical bubble volume in aqueous polyacrylamide (PAAm) solutions. The non-Newtonian solutions of 0.15, 0.20, 0.25 wt.%, Separan-AP-30, were made in a 50/50 wt.% demineralized water/glycerine mixture. The rheological characterization of the PAAm solutions was performed with an AR 1000-N rheometer (Rheolyst T.A. Instruments) for shear rates ranging from 0.1 to 1000 s^{-1}. The minimum measurable viscosity and normal stress, according to the equipment specifications, are 1×10^{-3} Pa s and 10 Pa, respectively. For the lower range of measurements, there is an uncertainty of up to 10%

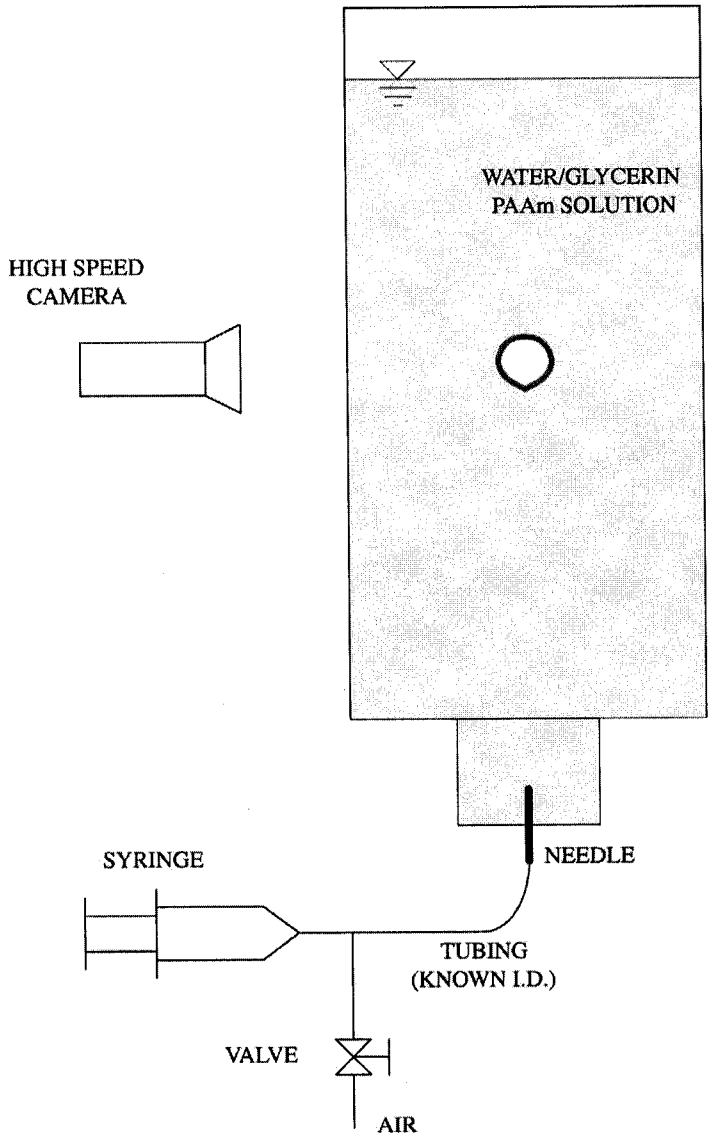

Fig. 2. A schematic representation of the experimental setup.

of the measured value. As can be seen in Fig. 1, the PAAm solutions are both shear thinning and viscoelastic.

These experiments were performed in the arrangement shown in Fig. 2 using plexiglass tanks 800 mm high with three different cross-sections (100 mm × 100 mm, 150 mm × 150 mm and 300 mm × 300 mm). We used these tanks to determine the wall effect in the discontinuity bubble velocity–volume. Air bubbles in a volume range from 5×10^{-9} to 100×10^{-9} m^3 were injected using a capillary tube centered at the bottom of the tank. The volume of the bubble was determined before injection to the tank by

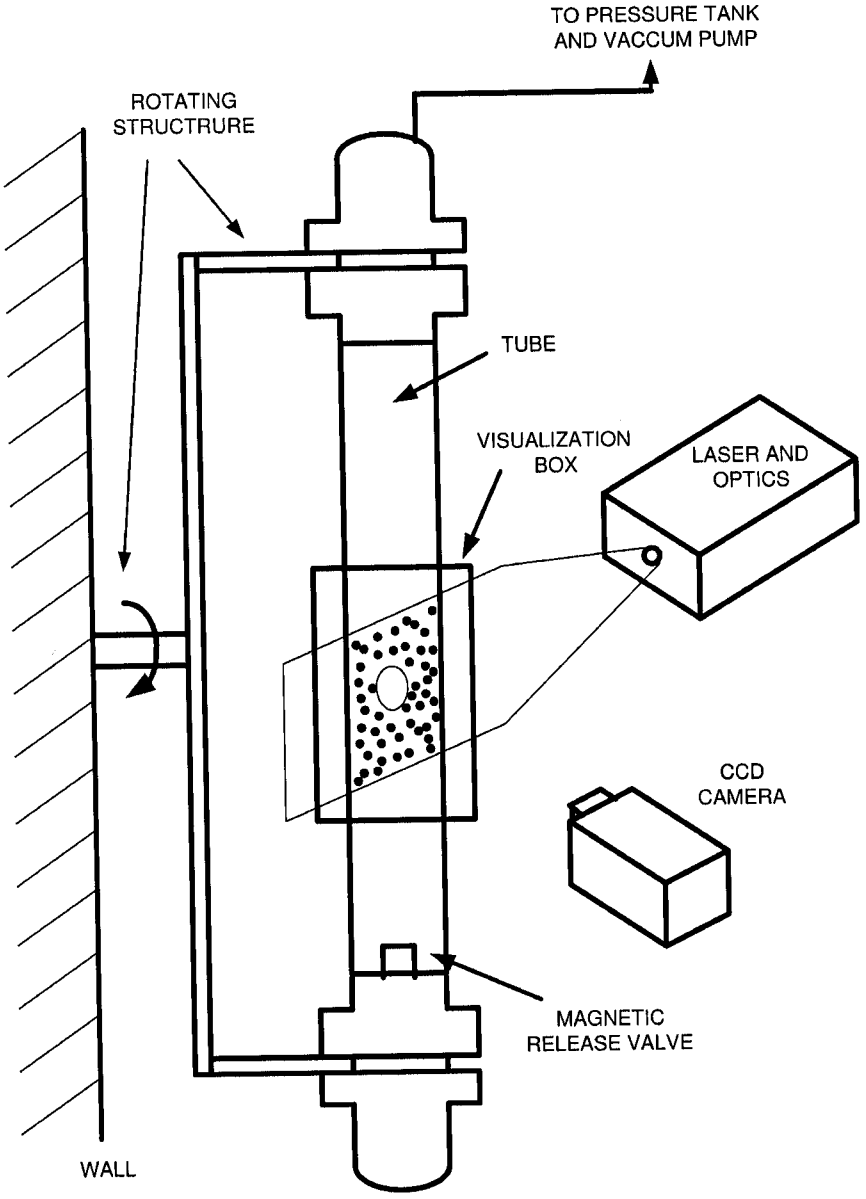

Fig. 3. Experimental setup with pressure control for the PIV measurements.

measuring its length trapped in a transparent capillary tube of a known inner diameter. The terminal bubble velocity was measured from consecutive digital images obtained using a high-speed camera (Kodak Motion Corder Model 1000, of up to 500 frames/s). The injection period was approximately of 300 s, to ensure the initial isotropic molecular configuration of the polymer [14]. The measurements were carried out at a location of $L/D \approx 100$, were L is the distance from the bottom and D the size diameter bubble.

Once the critical bubble volume was determined, the experiments to study the flow field generated around the rising bubble near the discontinuity were performed in a different setup, shown schematically on Fig. 3. A vertical glass tube with 50 mm internal diameter and 1500 mm high was filled with the non-Newtonian solution and inseminated with fluorescent polymer beads as seeding particles. To minimize the possible changes of the surface properties of the liquid–gas interphase, the tracer particles were thoroughly cleaned. They were initially rinsed once using HPLC isopropyl alcohol and two more times using pure water (18 MΩ/m). It must be noted that the rheological characterization (shown in Fig. 1) was performed on liquids without particle tracers. The flow field was illuminated by a green laser sheet (532 nm); the tracer particles fluoresced at this light wavelength. An orange filter was used in the camera to eliminate the reflections produced by the gas–liquid interface. In this way, only the fluorescent light of the tracer particles was visible. The measuring section was located at the mid-height of the tube, enclosed in a rectangular glass box filled with the aqueous solution in order to minimize the curvature effects of the pipe. A single bubble was injected in the tube with a volume close to where the jump discontinuity occurred. Different bubble volumes were obtained by controlling the pressure in the tube considering that, for the simplest case, the bubble volume is inversely proportional to the pressure. The terminal bubble velocity and the flow field around rising bubbles were determined on a plane crossing the axis of symmetry of the bubble using a PIV technique. The pressurized-tube could be rotated 180° around its center to *return* the air bubble to its original position where it was trapped using a magnetic valve. The same bubble was released and recovered for many experiments. This setup had two main advantages. First, the bubble volume could be carefully varied by changing the pressure of the tube. Second, the contamination of the fluid was minimized, since it was contained at all times inside the tube; hence, the presence of a free surface in contact with the ambient was avoided.

3. Results

3.1. Velocity jump

A series of experiments were conducted to investigate the effect of the PAAm concentration on the bubble velocity discontinuity. The non-Newtonian fluids used (0.15, 0.20, 0.25 wt.%, Separan-AP-30 with 50/50 wt.% demineralized water/glycerine mixture) exhibited a noticeable bubble velocity–volume discontinuity as a function of the PAAm concentration. Fig. 4 shows the bubble velocity–volume plot for the three solutions considered. These experiments were performed using a square Plexiglass tank of 800 mm high and a cross-section size of 100 mm × 100 mm.

We found that the terminal bubble velocity decreases as the PAAm concentration increases. The critical volume at which the jump was observed decreased as the concentration of polymer increased. Rodrigue et al. [8] did not observe a change of the critical volume as a function of the polymer concentration.

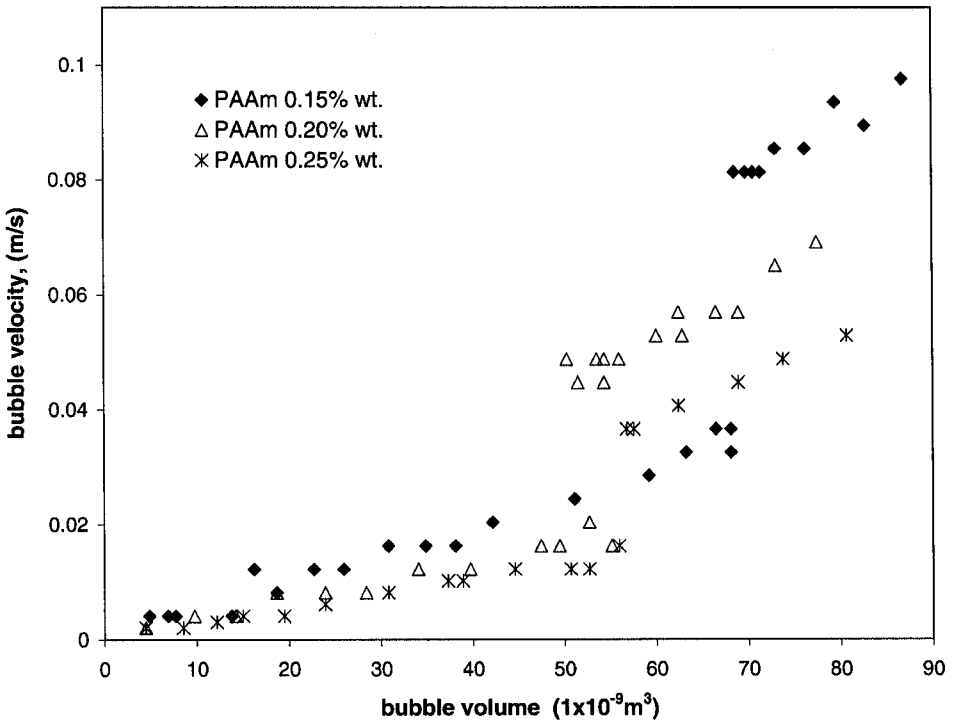

Fig. 4. The rising bubble velocity as a function of the bubble volume for three PAAm concentrations.

Also, we observed that the magnitude of the discontinuity, defined as the ratio of velocity increase to the velocity before the jump, increases slightly with the polymer concentration. This is in agreement with the observations by Rodrigue et al. [8]. Our results are summarized in Table 1.

3.2. *Wall effect*

The wall effect on the bubble velocity–volume discontinuity was obtained by performing experiments in three different size tanks. We considered only one PAAm solution (0.25 wt.% concentration). Fig. 5 shows the bubble velocity–volume plot for the three tanks considered. Clearly, the walls have a significant

Table 1
Summary of experimental results

Cross-section (mm^2)	PAAm solution (wt.%)	Volume (1×10^{-9} m^3)	V_b, before jump (m/s)	V_a, after jump (m/s)	$(V_a - V_b)/V_b$
100 × 100	0.15	68.2	0.036	0.081	1.25
100 × 100	0.20	53.1	0.018	0.044	1.44
100 × 100	0.25	56.3	0.016	0.037	1.31
150 × 150	0.25	58.8	0.036	0.068	0.88
300 × 300	0.25	59.2	0.065	0.121	0.86

Critical volumes and bubble velocities for all the cases studied.

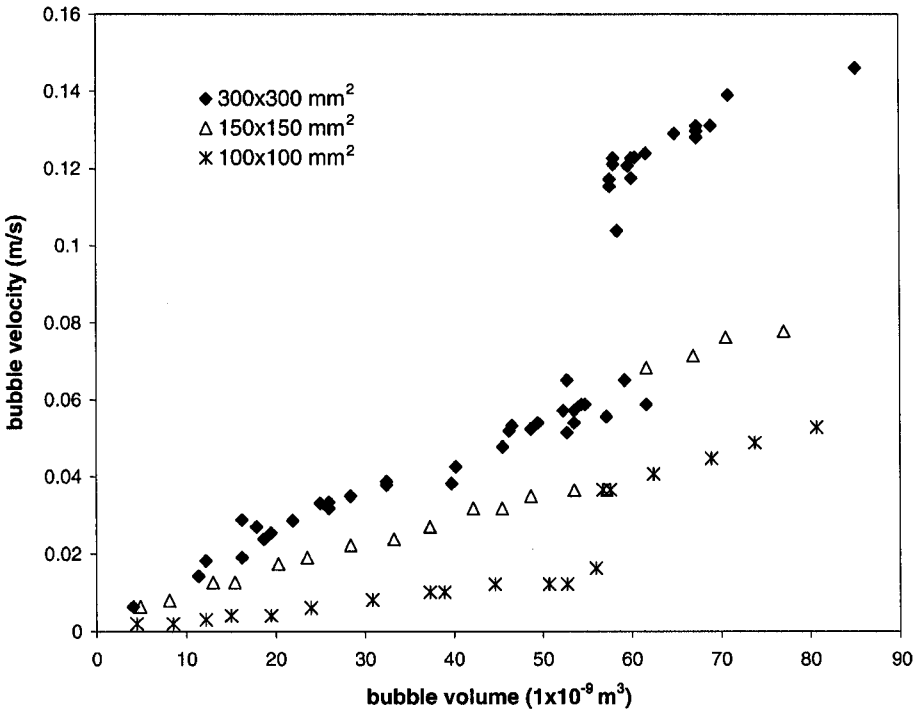

Fig. 5. The rising bubble velocity as a function of the bubble volume for the three tank sizes considered.

effect upon the results. The bubble velocities decrease with the size of the channel, but the critical bubble volume remains unchanged.

3.3. *Velocity fields around bubbles*

Flow fields around bubbles below and above the critical bubble volume were obtained for a 0.25 wt.% PAAm solution. The experiments were performed using the pressure-tube (Fig. 3) to obtain a better bubble volume control near the jump discontinuity. Fig. 6 shows a typical result obtained for the case when the bubble volume is below the critical bubble volume (55×10^{-9} m^3). The ruler shown to the left of the figure depicts the true scale of the graph in mm. Also, the length of the vectors was drawn using the same scale: a vector length of 1 mm corresponds to a velocity of 2 mm/s. For this case the rising velocity was 0.92×10^{-2} m/s and characterized by a local effective Reynolds number $Re_e = 0.5$ based on the local effective fluid viscosity [14].

The flow field is characterized by an upward flow in the front and back of the bubble with a quasi-symmetrical vortex surrounding the bubble. It is important to note the existence of a *positive wake*. For bubbles of this size we do not observe the appearance of the often-quoted *negative wake*. For this case the flow is similar to that observed around small bubbles in a Newtonian liquid.

For the case of a bubble with a volume above the critical volume (60×10^{-9} m^3), with rising bubble velocity of 3.9×10^{-2} m/s and a local effective Reynolds number of $Re = 2.5$, the velocity field changes drastically. In this case, an increased upward flow is observed and the *negative wake* appears (Fig. 7). The asymmetrical vortex structure is also observed in this case, but with an increased strength.

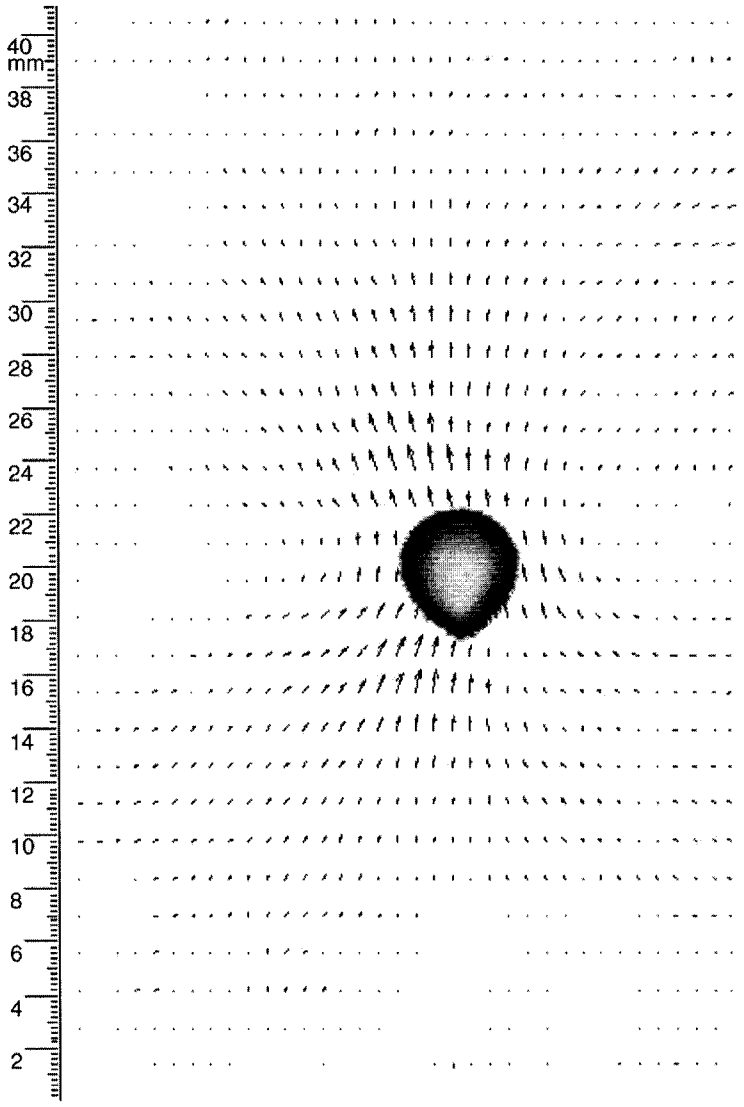

Fig. 6. Flow field velocity around a rising bubble in a 0.25 wt.% PAAm solution. For this case, the bubble volume is below the critical volume (55×10^{-9} m^3). The ruler shown to the left of the figure depicts the true graph scale in millimeters. The length of the vectors was drawn using the same scale: a length of 1 mm corresponds to a velocity of 2 mm/s.

Although only results for the 0.25 wt.% are shown, similar experiments were performed for the other two liquids. A similar change of the velocity field was observed.

Despite the fact that the flow field around the bubble is very different for bubbles below and above the critical volume, the shape of the bubbles does not change significantly. Fig. 8 shows a series of photographs of bubbles for increasing sizes, all obtained for the 0.25 wt.% liquid. The first three images (a, b and c) show typical bubbles for volumes below the critical value. The second set of images (d, e and f) show bubbles above the critical volume. Note that the shape develops from an oval shape (for the smallest volume) to a teardrop shape. The teardrop shape becomes more elongated as the size increases.

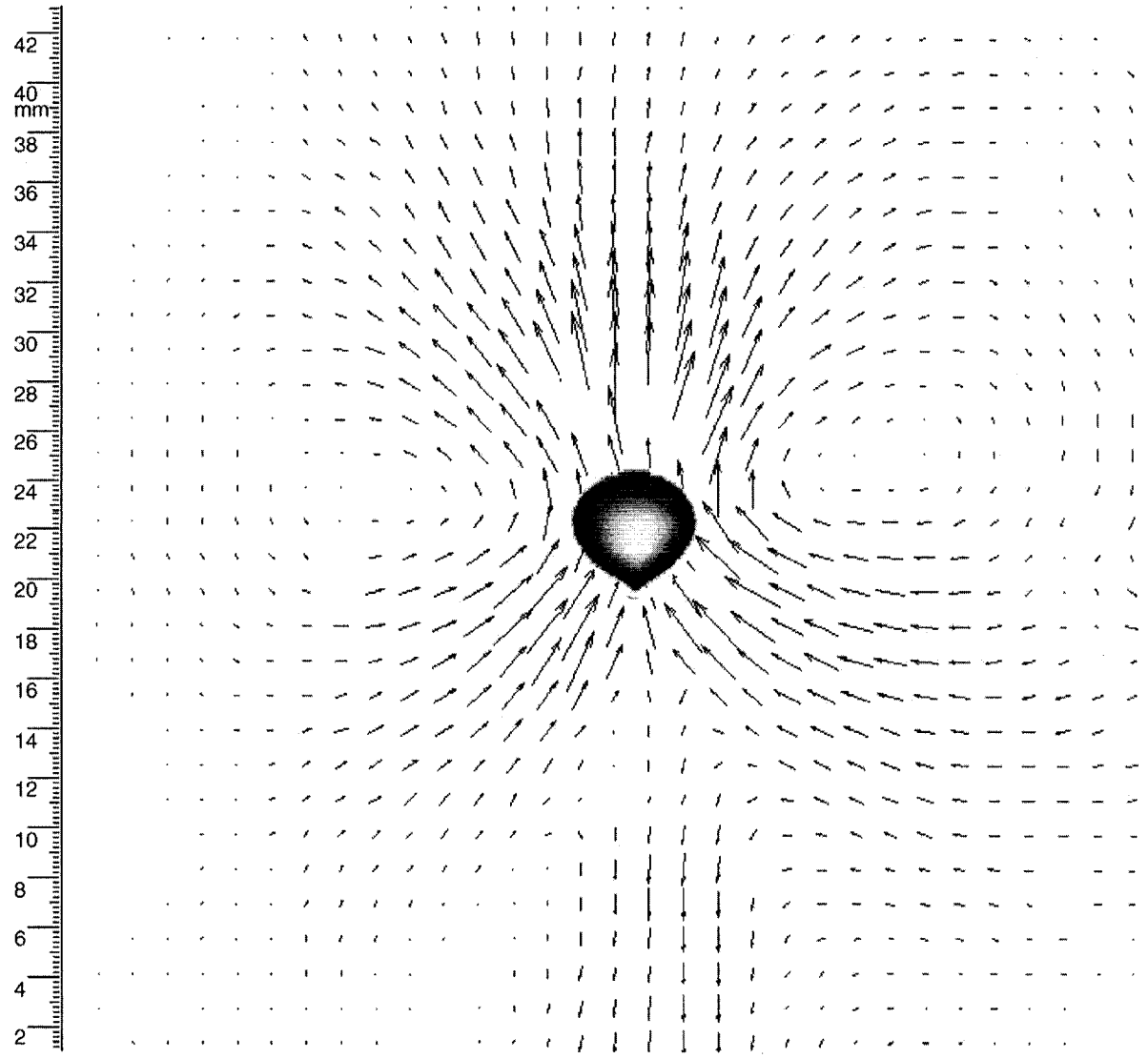

Fig. 7. Flow field velocity around a rising bubble in a 0.25 wt.% PAAm. For this case the bubble volume is above the critical volume (60×10^{-9} m^3). The ruler shown to the left of the figure depicts the true graph scale in mm. The length of the vectors was drawn using the same scale: a length of 1 mm corresponds to a velocity of 2 mm/s.

It may also be observed that the difference in shape between images (c) and (d) is very small (just below and above the critical volume). The first noticeable cusp appears for bubbles above the critical volume.

The appearance of the jump discontinuity and the *negative wake* cannot be explained only in terms of the bubble shape. We did not observed the extremely elongated bubbles shapes reported by Rodrigue et al. [15] for bubbles volume above the critical value. The formation of satellite bubbles, reported also by Rodrigue et al. [15], was observed only for bubbles larger than those studied here (i.e. volumes greater than 100×10^{-9} m^3).

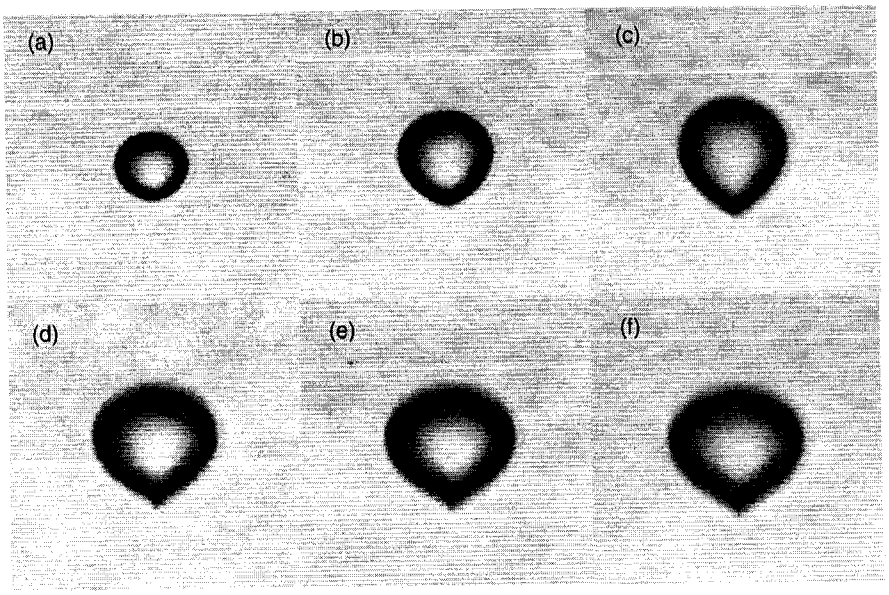

Fig. 8. Photographs of bubbles for volumes below and above the critical value: (a) 16 μl; (b) 32 μl; (c) 53 μl; (d) 67 μl; (e) 70 μl; (f) 85 μl.

4. Conclusions

We found that the viscoelastic properties of the non-Newtonian fluid and the container wall effects modify the bubble velocity and the critical bubble volume where the discontinuity of the bubble velocity occurs. An increase of the fluid elasticity results in a decrease in the magnitude of the bubble velocity and in a reduction of the critical bubble volume. The bubble velocity was found to decrease with container size even though the container was, in all cases, much larger than the bubble size. The critical bubble volume was not affected by the size of the container.

The most important contribution of this study is the determination of the flow field around the bubble for volumes above and below the critical bubble volume. The appearance of the so-called *negative wake* behind the rising bubble, appears only for bubbles sizes above the critical volume. We observed the existence of a vortex for bubbles larger and smaller than the critical volume. To our knowledge, the change of the flow configuration around the critical bubble volume has not been reported to date.

We conclude that the appearance of the negative wake is the main reason for the velocity jump to occur. Even though the change of the bubble shape is small, the appearance of the cusp for bubbles above the critical volume may also play an important effect. In addition, the shear thinning characteristics of the fluid may cause a local decrease of the viscosity resulting in an increase of the rise velocity. A combination of all these effects may cause the change from a positive to a negative wake behind the bubbles and may also originate the bubble jump discontinuity.

A complete explanation of the appearance of a negative wake for large bubbles in non-Newtonian fluids is not yet available. Further research is needed to investigate the dynamics around rising bubbles in viscoelastic fluids. Although a number of authors have observed the discontinuity in the velocity–volume curve, a fully quantitative explanation of its nature is still pending. The understanding of the phenomena

involved in the flow of individual bubbles is of fundamental importance to describe the rheology of systems with many bubbles. A sensible model to predict bubble interactions and coalescence rate in these systems is yet to be proposed.

Acknowledgements

The support of PAPIIT-DGAPA of UNAM through its Grant IN103900, and CONACYT through Grants NC-204 and J34497U-2 are greatly acknowledged. JRH-V wishes to acknowledge the Instituto Tecnológico de Zacatepec for its support during his postdoctoral stay at the IIM-UNAM. We thank E. Soto for his help in the rheological characterization of the liquids.

References

[1] R.B. Bird, C.F. Curtiss, R.C. Armstrong, O. Hassager, Dynamics of Polymeric Liquids, vol. I, second ed., Wiley, New York, 1989.
[2] R.P. Chhabra, Bubbles, Drops and Particles in Non-Newtonian Fluids, CRC Press, Boca Raton, 1993.
[3] D. Funfschilling, H.Z. Li, Flow of Non-Newtonian fluids around bubbles: PIV measurements and birefringence visualisation, Chem. Eng. Sci. 56 (2001) 1137.
[4] A.B. Metzner, E.A. Uebler, C.F. Chan Man Fong, Converging flow of viscoelastic materials, AIChE J. 15 (1969) 750.
[5] R.P. Chhabra, D. De Kee, Fluid particles in rheologically complex media, in: Transport Processes in Bubbles, Drops and Particles, Hemisphere, New York, 1992.
[6] O. Hassager, Negative wake behind bubbles in non-Newtonian liquids, Nature 279 (1979) 402.
[7] G. Astarita, G. Aapuzzo, Motion of gas bubbles in non-Newtonian liquids, AIChE J. 11 (1965) 815–820.
[8] D. Rodrigue, D. De Kee, C.F. Chan Man Fong, Bubble velocities: further developments on the jump discontinuity, J. Non-Newtonian Fluid Mech. 79 (1998) 45.
[9] D. Rogrigue, D. De Kee, C.F. Chan Man Fong, The slow motion of a single gas bubble in a non-Newtonian fluid containing surfactants, J. Non-Newtonian Fluid Mech. 86 (1999) 211.
[10] C. Bisgaard, O. Hassager, An experimental investigation of velocity fields around spheres and bubbles moving in non-Newtonian liquids, Rheol. Acta 21 (1982) 537.
[11] H.Z. Li, X. Frank, D. Funfschilling, Y. Mouline, Towards the understanding of bubble interactions and coalescence in non-Newtonian fluids: a cognitive approach, Chem. Eng. Sci. 56 (2001) 6419.
[12] G.M. Harrison, N.J. Lawson, D.V. Boger, The measurement of the flow around a sphere settling in a rectangular box using 3-dimensional particle image velocimetry, Chem. Eng. Commun. 188 (2001) 143.
[13] M.T. Arigo, G.H. McKinley, An experimental investigation of negative wakes behind spheres settling in a shear-thinning viscoelastic fluid, Rheol. Acta 37 (1998) 307–327.
[14] H.Z. Li, Y. Mouline, L. Choplin, N. Midoux, Rheological simulation of in-line bubble interactions, AIChE J. 43 (1997) 265.
[15] D. Rogrigue, D. De Kee, Bubble velocity jump discontinuity in polyacrylamide solutions: a photographic study, Rheol. Acta 38 (1999) 177–182.